Air Quality, Atmosphere & Health (2021) 14:411–429
https://doi.org/10.1007/s11869-020-00946-z

Application of satellite data and GIS services for studying air pollutants in Lithuania (case study: Kaunas city)

Arezoo Soleimany[1] · Raimondas Grubliauskas[2] · Vaida Šerevičienė[2]

Received: 8 July 2020 / Accepted: 28 September 2020 / Published online: 8 October 2020

Abstract

Satellite remote sensing, with its relatively short history, is going to play a major role in the fields that encompass topics related to place and space. Through this innovation in technology, real-time monitoring and mapping of changing phenomena on the surface of the earth has been possible. The purpose of this study was to investigate and evaluate the Kaunas city air pollutants between 14 and 25 October 2019 using environmental station data and satellite data (Terra, Aqua, OMI, and Sentinel-5P). The data obtained from satellite and the pollutant data gathered from air quality monitoring stations located in different parts of Kaunas were used. The data was downloaded for days mentioned above for the geographical bound of Kaunas city. Each data file covered an area of the size of Lithuania; hence, we should have extracted data for the area of interest, which was Kaunas city. The overall results of this study confirmed the capability of Sentinel-5P data to be used in monitoring the air quality and air pollution over the Kaunas local area. The existence of strong and acceptable correlations between satellite data and in situ measurements was indicative of the ability of satellite images to monitor air pollution, particularly over Kaunas urban areas during the fire incident in the city of Alytus.

Keywords Remote sensing · Air pollutants · Satellite data · Kaunas city

Introduction

Several studies conducted around the world have confirmed the adverse effects of air pollution on human health (Brunekreef and Holgate 2002; Hoek et al. 2013; Liu et al. 2013; Clark et al. 2014; Evans et al. 2014; Brook et al. 2017; Usmani et al. 2020). Monitoring environmental pollutants over urban areas using remote sensing methods is recommended to achieve sustainable development (Putrenko and Pashynska 2017). During the past 20 years, information about SO_2 and NO_2 vertical column density (VCD) and aerosol optical depth (AOD) has been collected by several satellites globally; such data are used to restrict estimation of emissions at different spatial resolutions (Wang et al. 2020).

✉ Arezoo Soleimany
arezoo_solimany@yahoo.com;
arezoo.soleimany@stu.malayeru.ac.ir

[1] Department of Environment, Faculty of Natural Resources and Environment, Malayer University, Malayer, Iran

[2] Department of Environment Protection and Water Engineering, Faculty of Environmental Engineering, Vilnius Gediminas Technical University, Vilnius, Lithuania

Controlling the air quality of cities through regulations would be an effective way provided that main areas are thoroughly monitored; thus, it is possible to quantify emissive pollutants and understand their chemical processes in the atmosphere. Satellite-based information and the measurements from either ground stationary bases or research aircraft form the major components of air-quality monitoring systems (Martin 2008; Duncan et al. 2014; Barkley et al. 2017). Measurements of some pollutants, including NO_2, formaldehyde (HCHO), CO, O_3, SO_2, and particulate matter (PM) using satellites, are commonly employed to determine the global distribution of the pollutants in the atmosphere, to measure surface precursor, and to assess the air quality of the area of concern (Martin 2008; Streets et al. 2013; Duncan et al. 2014; Barkley et al. 2017).

Albeit being new, satellite remote sensing is nowadays playing a key role in all fields with topics concerning place and space. Satellites are successfully utilized as devices for the evaluation of air quality in urban areas (Alston et al. 2011). Real-time observations and delineating of different ongoing events on the earth's surface have become possible via satellite remote sensing. This innovative technology has some brand advantages, including large-scale coverage, being effective through long study times, and relatively low cost. Thus, it is

referred to as one of the major methods for gaining information about the global distribution of aerosol (Gorelick et al. 2017).

Nowadays, large pieces of atmospheric composition satellite data are available for characterizing air quality (AQ) which are noteworthy to environmental professionals: sulfur dioxide (SO2), nitrogen dioxide (NO2), ammonia (NH3), carbon monoxide (CO), some volatile organic compounds (VOCs), and aerosol optical depth (AOD), from which surface particulate matter ($PM_{2.5}$) may be inferred.

The prediction ability of aerosol optical depth remote sensing has been extensively examined by researchers for $PM_{2.5}$ together with other meteorological and land-use variables (Liu et al. 2005; Liu et al. 2009). AOD measures the extent to which dust particles and aerosols obstruct solar beam from passing through the atmosphere. High resolution, global scale coverage, and universal accessibility are introduced as applied advantages of satellite-based AOD. Many types of research have been conducted on the relation between AOD and the PM (Koelemeijer et al. 2006; Chu et al. 2003; Emili et al. 2010; Rohen et al. 2011; Wang and Christopher 2003).

The most commonly used satellite data for the evaluation and determination of the concentration of PM around the earth is the aerosol optical depth, in which the integrated radiation scattering and the light absorbed by aerosols in an atmospheric column initiated from the earth surface and extended to the top of the atmosphere is revealed. AOD depends on the particles' mass concentration and size distribution; thus, it can be selected as a proxy for PM. Several approaches have been developed for the estimation of near-surface PM through columnar AOD (Chu et al. 2016).

Many types of research have been conducted on air pollution and studied the composition of pollutants using remote sensing, some of which are mentioned below. Tsai et al. (2011) examined the relationship between the optical light damage data of MODIS and the concentration of suspended particles for a given period. Their results revealed the high ability of the sensor to observe suspended particles. Bechle et al. (2012) compared the satellite and terrestrial data for NO_2. Using OMI images, they obtained NO_2 concentration at low levels and used this data for investigating NO_2 contamination in different urban areas. Tatem et al. (2004) studied epidemiology and public health effects of aerosols and PM using Terra and Aqua MODIS data. High-resolution Aster data was employed in their study for analysis of boundaries for different amounts of pollutants. There are some literatures in which satellite trace gas measurements were used to study air pollution trends (Richter et al. (2005), van der et al. (2006, 2008), Ghude et al. (2008), De Smedt et al. (2010, 2015), Russell et al. (2012), Schneider and van der (2012), Hilboll et al. (2013), Jin and Holloway (2015), Krotkov et al. (2016), Lamsal et al. (2015), Lelieveld et al. (2015), Schneider et al. (2015), Duncan et al. (2016), and Barkley et al. (2017)).

A fire broke out in one of the biggest tire recycling factories in the Baltics in the early hours on 16 October in Alytus, a town in southern Lithuania. Strong southward winds blew the smoke towards a nearby residential block of Alytus, a town of about 55,000 populations. According to reports, the smoke was felt a dozen kilometers from the fire.

Kaunas is located in Lithuania with latitude = 54.898903 and longitude = 23.885275 coordinates. The calculated flying distance from Alytus to Kaunas is equal to 35 mi (56 km). The driving distance between Alytus and Kaunas is 70.41 km. Since pollutants can stay in the atmosphere from a few minutes until years, although they are often a local problem, they can affect larger areas such as a country. Therefore, due to the importance of the fire issue for the environment, climate, and air of nearby Alytus cities like Kaunas city and the relatively short distance between the two cities of Kaunas and Alytus, in this study, we tried to investigate air pollutants during 12 days.

The purpose of this study was to investigate and evaluate the Kaunas city air pollutants between 14 and 25 October 2019, when the tire recycling manufactory fire occurred in the Alytus, using environmental station data and satellite data (Terra, Aqua, OMI, and Sentinel-5P). With this background in mind, in this study, we explored the accuracy of air pollutants from different satellite data and AOD products from the Moderate Resolution Imaging Spectroradiometer (MODIS) and Aerosol Index (AI) from Sentinel-5P (OFFL/NRTI) and OMI(Aura). Also, we studied the relationship between different air pollutants and in situ measured concentration in the Kaunas city.

Materials and method

Study area

Kaunas is the second largest city in Lithuania with a total population of 289,380. Kaunas is located in the central part of Lithuania on the confluence of the two largest Lithuanian rivers, namely, the Nemunas and the Neris; therefore, the city has excellent opportunities for the development of water transport. Kaunas is located in a 100-km distance from the capital city of Vilnius and 212 km from the country's major seaport, Klaipeda. The city is also located at the crossroads of the country's two major motorways: the A1 motorway, Vilnius–Kaunas–Klaipeda, a connection between the capital city of Vilnius and the ice-free Klaipėda Seaport. The Via Baltica (road E67) beginning from Estonia, crossing Latvia and Poland, which ends in Czechia is integrated into the Trans-European motorway system and connects Nordic countries to Central and Western Europe. Kaunas region is one of the most important regions in Lithuania. There are 8 municipalities in the Kaunas region, compactly situated around the administrative center—Kaunas city. The Region comprises the city of Kaunas, Birstonas town, and the districts of Kaunas,

Kaisiadorys, Prienai, Raseiniai, Kedainiai, and Jonava with a population of 673 thousand. Kaunas region is the central region in the country. It is the geographical, educational, industrial, and transport center of Lithuania (Fig. 1).

The data used in this study were divided into two sections: ground data and satellite data.

Air pollutants data from ground-based stations

Ground data include air pollution data measured at Kaunas city air quality monitoring stations. In this study, data from two Kaunas air quality monitoring stations were used. These stations are measuring the number of pollutants such as carbon monoxide, sulfur dioxide, nitrogen dioxide, ozone, and particulate matter hourly during the day and night. The data were used as a reference to reflect the differences in pollution levels at different types of stations.

Satellite data

The NASA Giovanni data analysis system is a well-known and useful tool for analyzing various types of remote sensing data. Air quality is a concern in public health. Aerosol optical depth data products, which are acquired by MODIS and the ozone measuring instrument (OMI), are probably the most commonly accessed air quality-related data in Giovanni. The optical clarity of the atmospheric air column is indicated by AOD, where higher AOD values suggest that atmospheric particles and chemicals are more scattered and absorbed by atmospheric particles and chemicals. Due to the correlation

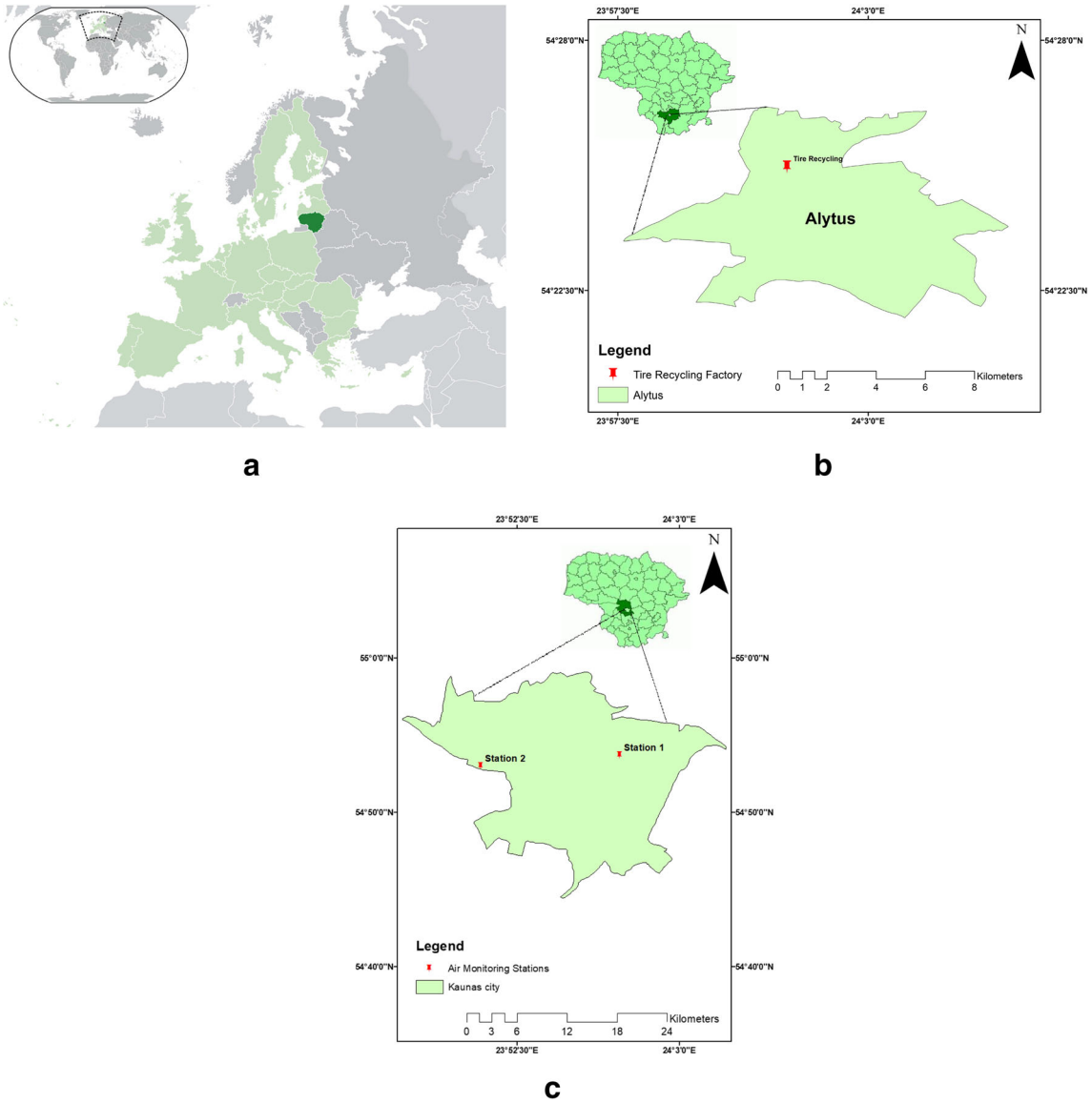

Fig. 1 (**a**) Location of Lithuania country on the world. (**b**) Location of Alytus and tire recycling factory. (**c**) Study area and location of air quality monitoring stations in Kaunas city

between AOD and $PM_{2.5}$ and PM_{10}, several various studies have used AOD data variables as their data resources. Prados et al. published a comprehensive review of the use of air quality-related data sets in Giovanni (Prados et al. 2010).

Some data on the chemistry of the atmosphere are obtained through OMI. The harmful effect of ozone layer depletion on human health is clear; thus, OMI ozone data are used in such researches. By monitoring nitrogen NO_2 data collected by OMI, it would be possible to track any wildfire location. OMI portal also provides access to NO_2, SO_2, and CH_2O columns of the troposphere. It has been reported that the NO_2 column measurements by OMI are more sensitive to boundary layer concentrations over the USA than those obtained from ground-based networks (Celarier et al. 2008; Lamsal et al. 2008). Similarly, SO_2 measurements are shown to be sensitive to the boundary layer over larger time scales (Carn et al. 2007; Krotkov et al. 2008).

OMI level 3 trace gas products are on a 0.25 × 0.25-degree grid and have the added advantage of being available at higher spatial resolution than level 3 aerosol products at 1 × 1-degree resolution. This makes the datasets more suitable for monitoring urban scale pollution. There is also an experimental NASA product that will soon be providing OMI columns at 0.05 × 0.05-degree resolution. The users can analyze time series and multi-day area-averaged image maps using Giovanni, with no need for downloading the software (Prados et al. 2010; Duncan et al. 2014).

MODIS Deep Blue aerosol product

In this study, the MODIS Deep Blue (DB) algorithm was employed to extract the aerosol optical depth (AOD) and estimate the concentration of particulate matter. It uses the radiance measurements at 412 nm (blue wavelength), in which the land surface reflectance is lower than the reflectance at longer visible wavelengths, to retrieve the column AOD over bright surfaces and vegetated areas, as well (Hsu et al. 2004; Hsu et al. 2013). In the DB surface characterization procedure, the dynamic surface reflectance method for urban zones and the precalculated surface reflectance database are combined with the normalized vegetation index in arid and semiarid areas (King et al. 1992; Hsu et al. 2013). The dynamic surface reflectance method allows larger spatial coverage of the DB aerosol product by expanding the retrieval capability from the bright surfaces to all snow-free land surfaces, including vegetated areas. The surface reflectance dataset used in the DB algorithm was created from the full-time series and revised during each reprocessing (Hsu 2017).

Sentinel 5P

The first Copernicus mission for monitoring the atmosphere is called the Sentinel-5 Precursor. As air pollution has become a main global concern, Copernicus carries the Tropomi instrument which can map a multitude of trace gases which may affect the air quality and climate, including nitrogen dioxide, ozone, formaldehyde, methane, carbon monoxide, and aerosols (Slagter et al. 2020; Safarianzengir et al. 2020). The datasets provide near real-time (NRTI) and offline (OFFL) versions.

Google Earth Engine is an Internet-based platform that provides satellite imagery, time-series data, cloud-based computing, and access to software and processing algorithms for such data (Gorelick et al. 2017; El-Nadry et al. 2019; Chen et al. 2020). In this study, we used the Google Earth Engine (GEE) tool to process the air quality datasets of TROPOMI products, including OFFL NO_2 (NO2_*column_number_density* in the unit of mol/m^2), OFFL SO_2 (S*O2_column_number_density* in the unit of mol/m^2), NRTI NO_2, and NRTI SO_2 column densities (*NO2_column_number_density* and S*O2_column_number_density_amf*) (mol/m^2), and NRTI & OFFL Ultraviolet (UV) Aerosol Index (UVAI), whose negative or small values represent non-absorbing aerosols, while larger positive values represent absorbing aerosols (e.g., dust) (*absorbing_aerosol_index* as unitless).

Using the Google Earth Engine tools and through the coding we did, the average NO_2 concentration, SO_2 concentration, and Aerosol Index (AI) values over Kaunas city in the period of 14–25 October 2019 were downloaded and statistically processed. For the whole Kaunas city, we extracted the sum, minimum, maximum, and mean of the NO_2, SO_2, and Aerosol Index. Units of nitrogen dioxide (NO_2) and sulfur dioxide (SO_2) contaminants were converted from moles per square meter (mol/m^2) to micrograms per cubic meter (μg/m^3). After that, distribution maps of pollutants were drawn using GIS software.

Various satellite data, such as Sentinel-5P, Aura/OMI, and MODIS (Terra and Aqua), were used to estimate the concentration of various air pollutants including NO_2, SO_2, particulate matter ($PM_{2.5}$ and PM_{10}), and AI as well. All products were extracted for each day and each ship position corresponding to ground-based measurements. The relations between all parameters were statistically examined using correlation and regression analysis in SPSS (version 22) statistical analysis software. Also, all distribution maps and spatial analyses were performed in ArcMap/GIS 10.3 software.

Accuracy results

One of the criteria for validating the results obtained from the models is the determination coefficient (R^2). The R^2 is used as an indicator to express the accuracy of the regression line, and its value varies between zero and one, indicating values close to a better match of the observed and estimated data. However, since the value of R^2 is affected by discarded data,

other parameters must be used as well. For this reason, other parameters such as the root mean square error (RMSE) and the mean absolute error (MAE) are also used to check the validity of the results. The root mean square error (RMSE) and the mean absolute error (MAE) are calculated as follows:

$$RMSE = \sqrt{\frac{1}{N}\sum_{n=1}^{N}[(m_i - o_i)]^2} \quad (1)$$

$$MAE = \frac{1}{N}\sum_{n=1}^{N}|m_i - o_i| \quad (2)$$

m_i and o_i are extracted data from satellites and measurement data, respectively, and N is the number of data. The MAE and the RMSE can be used together to diagnose the variation in the errors in a set of forecasts. The RMSE will always be larger than or equal to the MAE; the greater difference between them, the greater the *variance* in the individual errors in the sample. If the RMSE = MAE, then all the errors are of the same magnitude. Both the MAE and RMSE can range from 0 to ∞. Lower values are better. The low RMSE value and the high R^2 coefficient indicate the acceptable accuracy of the model and its superiority over the other models. MAE shows the difference between observational and computational data in a way that the lower the value, the more effective the work.

Results and discussion

The spatial distribution of pollutant concentrations from Sentinel-5P is presented in Fig. 2. The SO_2 concentration is higher in north, northeast, and northwest parts as well as parts of the center and southeast. NO_2 concentration is higher in the northern and especially northeastern parts, while it is lower in the southern parts and some parts of the northwest area. In the case of the AI, it is higher in the northern, northeastern, and northwestern parts as well as parts of the center and western parts, while it is lower in parts of the south and southeast.

Comparison of Sentinel-5P SO_2, NO_2, Aerosol Index, and in situ measurements

Air pollutants from satellite and in situ measurements are illustrated in Figs. 3, 4, 5, 6, 7, 8, 9, 10, 11, 12, 13, 14, 15, 16, 17. A strong linear relationship was found between Sentinel-5P (both of OFFL and NRTI) air pollutants and in situ measurements (Figs. 4, 6, 8, 10, 11, 13, 15, and 17).

Figures 3 and 5 show changes in the concentration of SO_2 contaminants over the period from October 14 to October 25. According to the pictures, with an increase in measured SO_2, the amount of SO_2 concentration extracted from the Sentinel-5P satellite also increased, while in situ SO_2 concentration was reduced by decreased Sentinel-5P's SO_2 concentration. In illustrating the changes of the pollutant in the study period, NRTI and OFFL data good and similar performance. A comparison of the values of the calculated accuracy indicators also confirms this (Figs. 4 and 6). This indicates that the Sentinel-5P NRTI and OFFL satellite data have been able to show the SO_2 pollutant concentration well.

Figures 7 and 9 show changes in the concentration of NO_2 contaminants over the period from October 14 to October 25. It could be seen that with the increment of measured NO_2, the amount of NO_2 concentration extracted from the Sentinel-5P satellite also increased, while in situ NO_2 concentration was reduced by decreased Sentinel-5P's NO_2 concentration. Both NRTI and OFFL data could properly show the changes of NO_2 pollutants in the mentioned period, although a comparison of the accuracy indicator values (Figs. 8 and 10) showed that the accuracy of OFFL data is higher than NRTI.

Linear regression analysis was performed to find the correlation between the Sentinel-5P (OFFL and NRTI) retrieved SO_2 and NO_2 values and in situ SO_2 and NO_2 concentration, and the resultant equations were as follows:

$$SO_{2\ In-Situ} = 5.005 + 0.160 * SO_{2\ Sentinel-5P/OFFL} \quad (3)$$

$$SO_{2\ In-Situ} = 4.981 + 0.160 * SO_{2\ Sentinel-5P/NRTI} \quad (4)$$

$$NO_{2\ In-Situ} = 7.917 + 0.663 * NO_{2\ Sentinel-5P/OFFL} \quad (5)$$

$$NO_{2\ In-Situ} = 6.385 + 0.661 * NO_{2\ Sentinel-5P/NRTI} \quad (6)$$

Simple linear regression was carried out to investigate the relationship between Sentinel-5P (OFFL and NRTI) retrieved SO_2 and NO_2 values (μg/m^3) and in situ SO_2 and NO_2 concentration (μg/m^3). The scatterplot (Figs. 4, 6, 8, and 10) showed that there was a strong positive linear relationship between the two, which was confirmed with Pearson's correlation coefficient of 0.953 and 0.951 for SO_2 Sentinel-5P (OFFL and NRTI) and 0.920 and 0.940 for NO_2 Sentinel-5P (OFFL and NRTI), respectively. Simple linear regression showed a significant relationship between Sentinel-5P (OFFL and NRTI) retrieved SO_2 and NO_2 values and in situ SO_2 and NO_2 concentration ($p < 0.001$). The slope coefficient for in situ SO_2 and NO_2 concentration were 0.160, 0.160, 0.661, and 0.663, so the Sentinel-5P (OFFL and NRTI) retrieved SO_2 and NO_2 values increases by 0.160, 0.160, 0.661, and 0.663 μg/m^3 for each extra μg/m^3 of in situ SO_2 and NO_2 concentration (Eqs. 3, 4, 5, and 6). The R^2 values were 0.91, 0.9042, 0.8459, and 0.8835 (SO_2 (OFFL and NRTI) and NO_2 (OFFL and NRTI), respectively) so 91%, 90.42%, 84.59%, and 88.35% of the variation in in situ SO_2 and NO_2 concentration can be explained by the model containing only SO_2 and NO_2 Sentinel-5P (OFFL and NRTI).

According to the results in Figs. 12, 14, and 16, as the amount of Aerosol Index (AI) extracted from the Sentinel-5P (NRTI and OFFL) images increased, the concentration of the particulate matter ($PM_{2.5}$ and PM_{10}) increased and

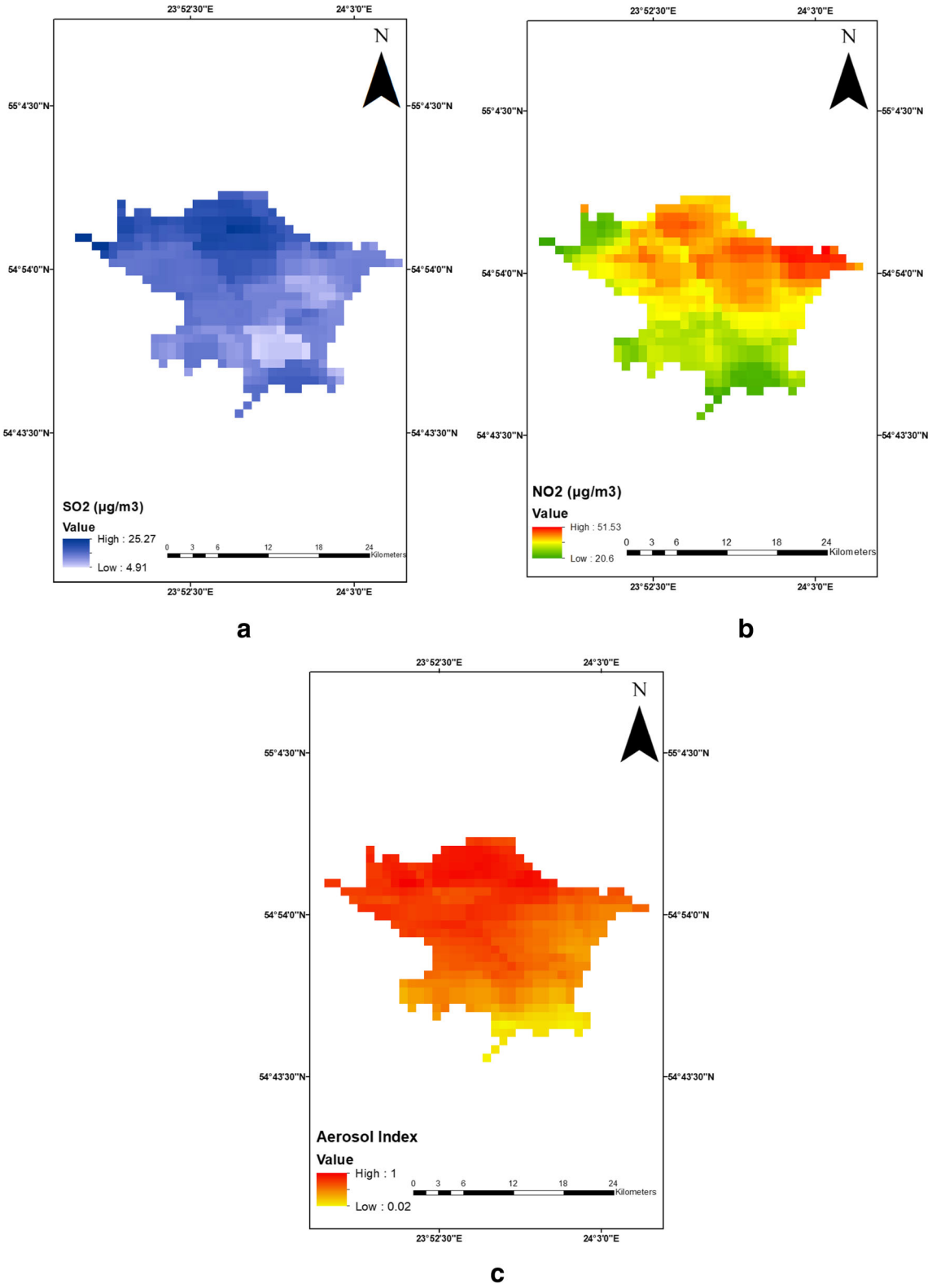

Fig. 2 Spatial distribution of the (**a**) SO_2 concentration, (**b**) NO_2 concentration, and (**c**) Aerosol Index (Sentinel-5P) from 14 to 25 October 2019 at Kaunas city

decreased as AI decreased. In estimating the concentration of particulate matter ($PM_{2.5}$), the Sentinel-5P NRTI data performed better than the OFFL data. For instance, on October 25, when the pollutant concentration was maximum, the AI extracted from the NRTI satellite image was also maximum (Figs. 14 and 15). This indicates that the

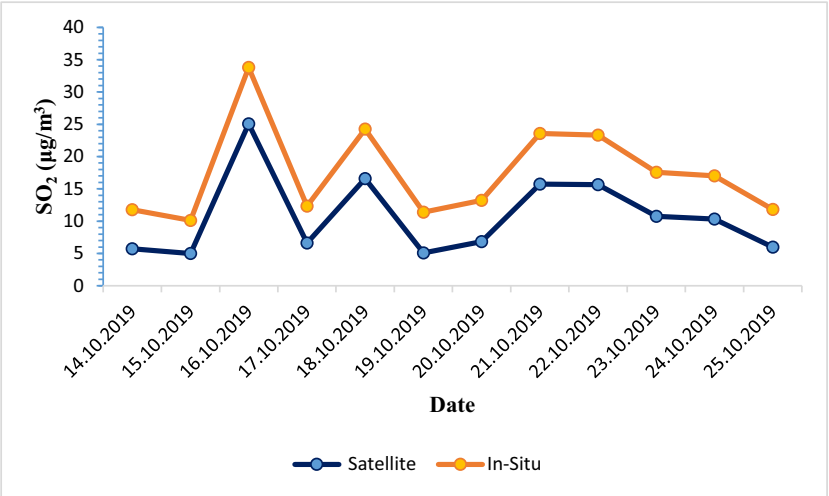

Fig. 3 Satellite (Sentinel-5P/OFFL) SO_2 and in situ SO_2 concentration

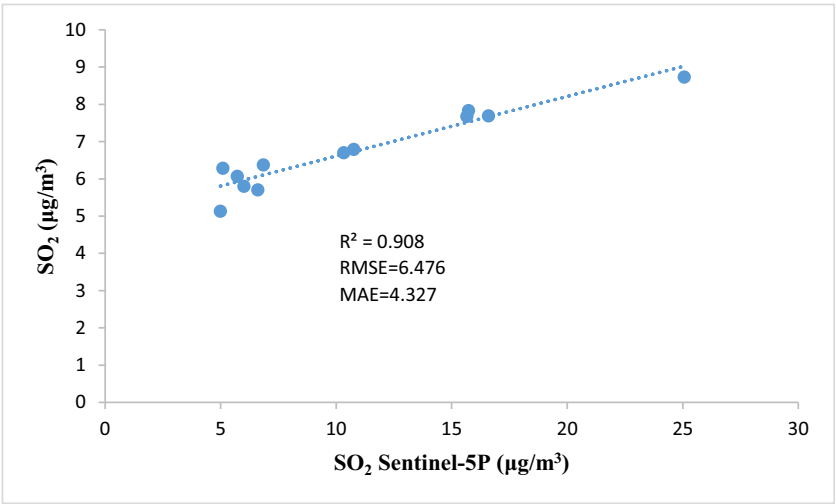

Fig. 4 Linear relation of Sentinel-5P/OFFL SO_2 and in situ SO_2 concentration

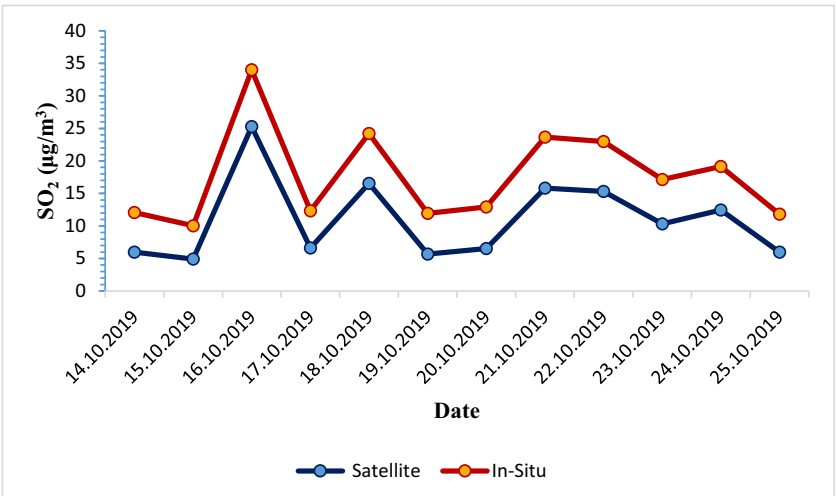

Fig. 5 Satellite (Sentinel-5P/NRTI) SO_2 and in situ SO_2 concentration

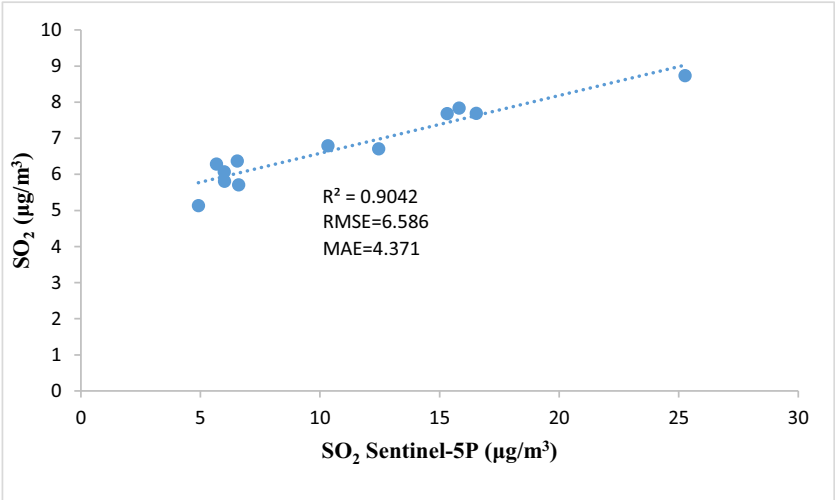

Fig. 6 Linear relation of Sentinel-5P/NRTI SO_2 and in situ SO_2 concentration

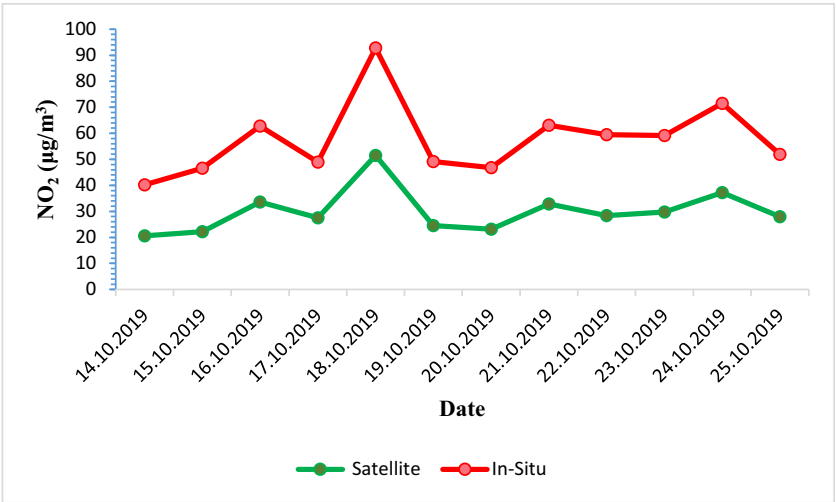

Fig. 7 Satellite (Sentinel-5P/OFFL) NO_2 and in situ NO_2 concentration

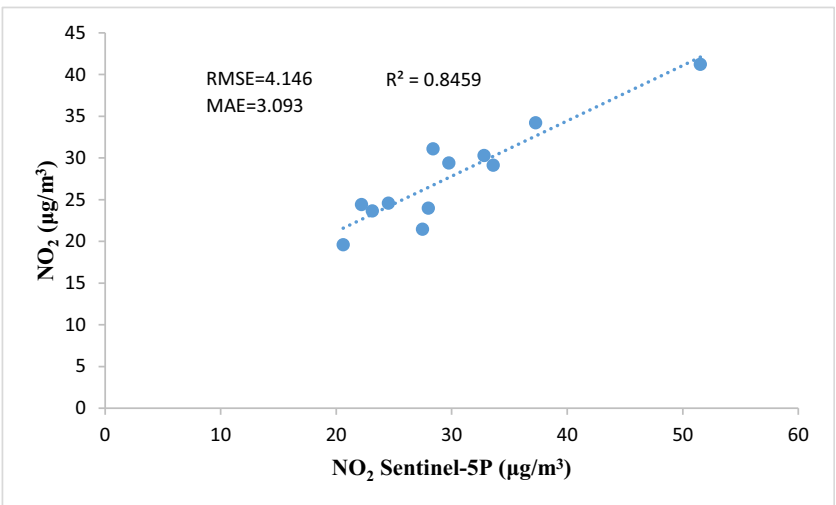

Fig. 8 Linear relation of Sentinel-5P/OFFL NO_2 and in situ NO_2 concentration

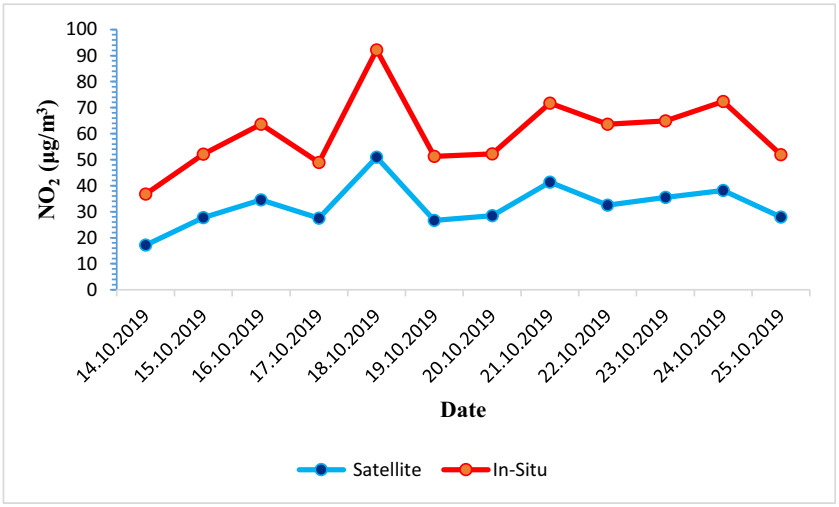

Fig. 9 Satellite (Sentinel-5P/NRTI) NO_2 and in situ NO_2 concentration

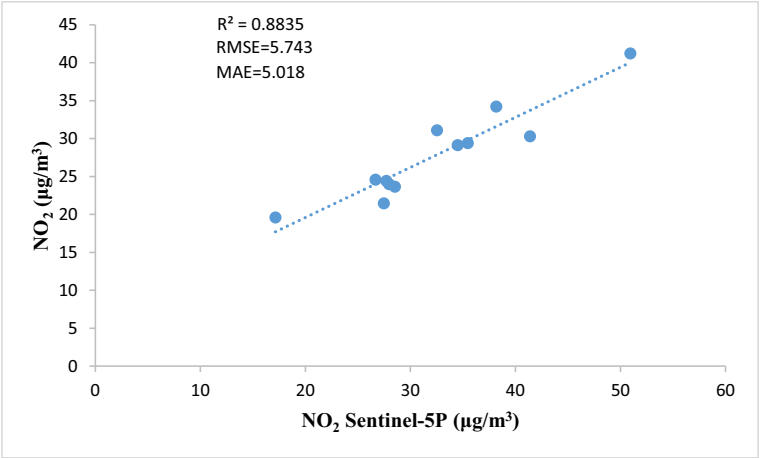

Fig. 10 Linear relation of Sentinel-5P/NRTI NO_2 and in situ NO_2 concentration

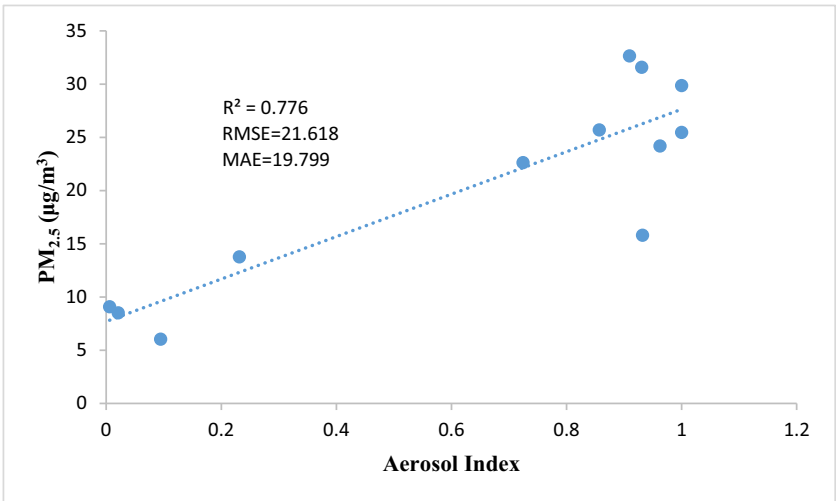

Fig. 11 Linear relation of Sentinel-5P/OFFL Aerosol Index and in situ $PM_{2.5}$ concentration

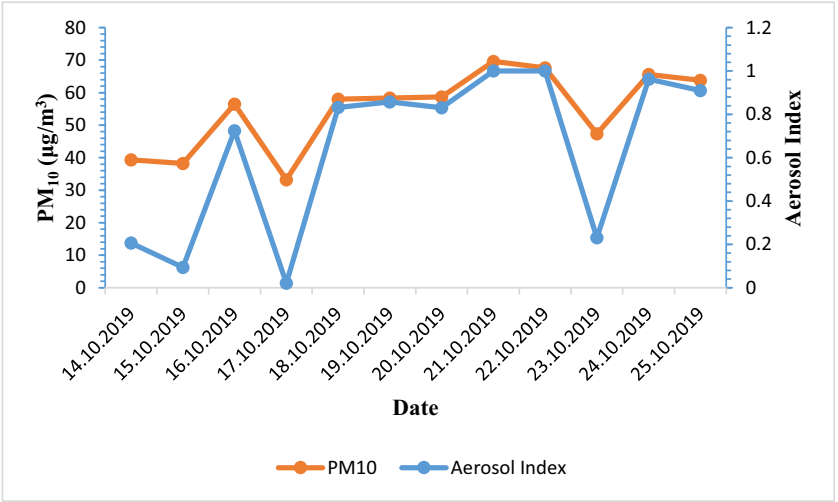

Fig. 12 Satellite (Sentinel-5P/OFFL) Aerosol Index and in situ PM_{10} concentration

Sentinel-5P NRTI satellite data has been able to show the $PM_{2.5}$ pollutant concentration well. Due to the proximity of RMSE and MAE values (Figs. 11 and 15), the validation was performed based on the determination coefficient (R^2), which confirms the above result. However, for estimating particulate matter (PM_{10}), both versions of Sentinel-5P (NRTI and OFFL) performed equally well (Figs. 12 and 16). Figures 13 and 17 also confirm this by revealing a very strong relationship and a high coefficient of determination.

The strong correlation between the AI values from the Sentinel-5P NRTI version and PM_{10} measurements in Kaunas city (Fig. 17) suggests that AI could be employed as a useful product for evaluating air quality and prediction of particulate matter (PM_{10}).

Also, the linear regression analysis was performed to find the correlation between the Sentinel-5P (OFFL and NRTI) retrieved AI values and PM (PM_{10} and $PM_{2.5}$) observations, giving the following equations:

$$PM_{10} = 36.603 + 28.307*AI_{Sentinel-5P/OFFL} \quad (7)$$

$$PM_{2.5} = 7.697 + 19.937*AI_{Sentinel-5P/OFFL} \quad (8)$$

$$PM_{10} = 34.679 + 37.257*AI_{Sentinel-5P/NRTI} \quad (9)$$

$$PM_{2.5} = 6.382 + 26.165*AI_{Sentinel-5P/NRTI} \quad (10)$$

A simple linear regression was calculated to predict in situ PM_{10} and $PM_{2.5}$ concentration based on AI values from Sentinel-5P (OFFL and NRTI). Significant regression equations were found ($F(1,10) = 122.107, p < 0.001$), with an R^2 of 0.924 for PM_{10} and AI(OFFL), ($F(1,10) = 470.704$, $p < 0.001$), with an R^2 of 0.979 for PM_{10} and AI (NRTI), ($F(1,10) = 34.635$, $p < 0.001$), with an R^2 of 0.776 for $PM_{2.5}$ and AI (OFFL), and ($F(1,10) = 44.753$, $p < 0.001$), with an R^2 of 0.817 for $PM_{2.5}$ and AI (NRTI). PM_{10} concentration increased 28.307 and 37.257 for each of AI (OFFL) and AI (NRTI), respectively (Eqs. 7 and 9). $PM_{2.5}$ concentration

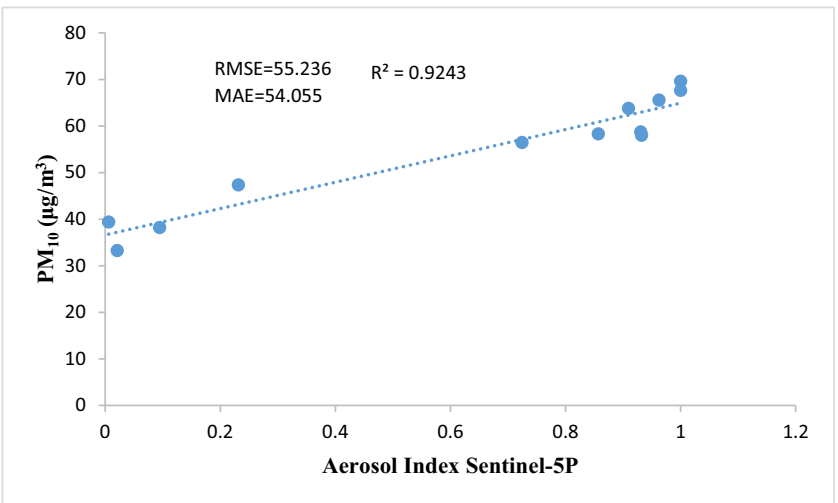

Fig. 13 Linear relation of Sentinel-5P/OFFL Aerosol Index and in situ PM_{10} concentration

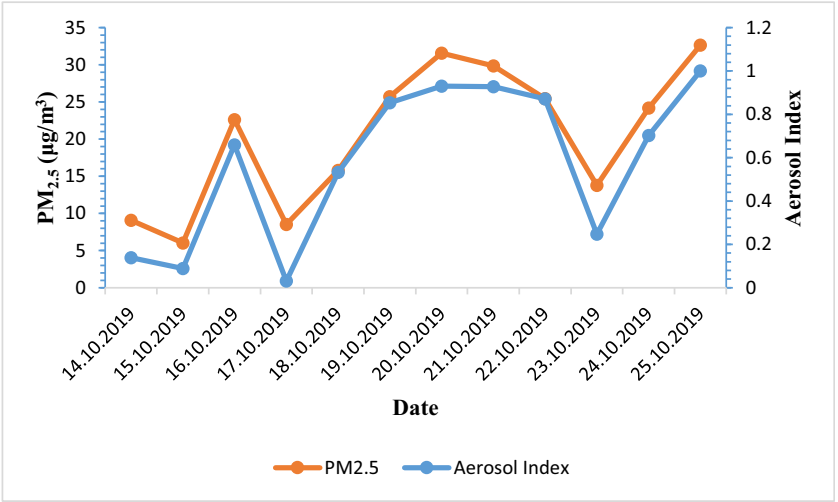

Fig. 14 Satellite (Sentinel-5P/NRTI) Aerosol Index and in situ $PM_{2.5}$ concentration

increased 19.937 and 26.125 for each of AI (OFFL) and AI (NRTI), respectively (Eqs. 8 and 10).

Figure 18 shows the spatial distribution of pollutant concentrations from Aura/OMI. The SO_2 concentration is higher in the northern, northeastern, and northwestern parts. NO_2 concentration is higher in the western half, while it is lower in the north, some parts of the northwest, eastern-half, and southeast parts. For the AI, it is higher in the south and southwestern parts and some parts of the northwest, while lower in the east.

Comparison of Giovanni AOD MODIS (Aqua and Terra) and in situ measurements

Aerosol optical depth (AOD) is one of the atmospheric products of the MODIS sensor that is used together with ground-based station information to predict the concentration of particulate matter. Accordingly, the concentration of particulate matter can be obtained in the areas where ground stations are not available. Figures 19, 20, 21, and 22 show the linear relationship between the AOD extracted from the Terra and Aqua satellite images and in situ measured $PM_{2.5}$ and PM_{10} concentration. As it is shown in the figures, a strong linear relationship was found between MODIS/Aqua, MODIS/Terra, and PM measurements.

Linear regression analysis was performed between the MODIS (Aqua and Terra) retrieved AOD values and PM ($PM_{2.5}$ and PM_{10}) observations and the following equations obtained:

$$PM_{10} = 32.441 + 249.807*AOD_{MODIS/Aqua} \quad (11)$$

$$PM_{2.5} = 2.771 + 198.320*AOD_{MODIS/Aqua} \quad (12)$$

$$PM_{10} = 33.118 + 212.747*AOD_{MODIS/Terra} \quad (13)$$

$$PM_{2.5} = 2.703 + 174.882*AOD_{MODIS/Terra} \quad (14)$$

A simple linear regression was carried out to test if AOD values significantly predicted PM ($PM_{2.5}$ and PM_{10})

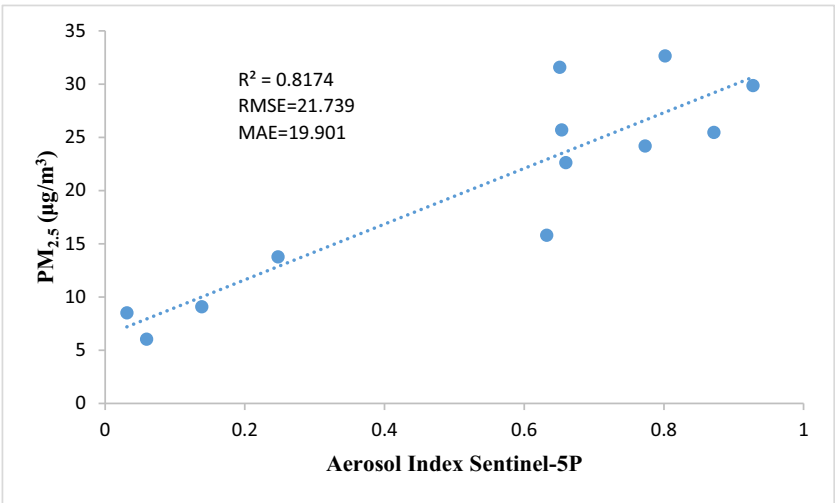

Fig. 15 Linear relation of Sentinel-5P/NRTI Aerosol Index and in situ $PM_{2.5}$ concentration

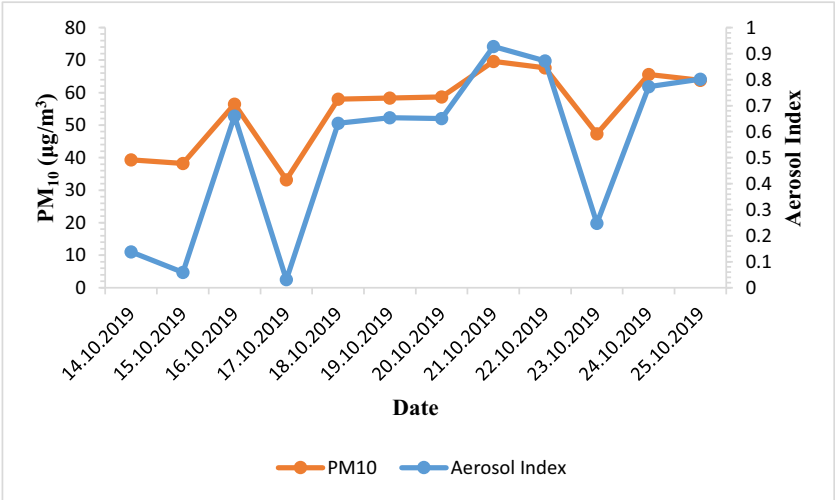

Fig. 16 Satellite (Sentinel-5P/NRTI) Aerosol Index and in situ PM_{10} concentration

observations. The results of the regression between PM_{10} and AOD (Aqua and Terra) indicated that the models explained 84.4% and 80% of the variance and that the models were significant, $F(1,10) = 54.279$, $p < .001$ and $F(1,10) = 40.120$, $p < .001$, for PM_{10} & AOD (Aqua) and PM_{10} &AOD (Terra), respectively. It was found that AOD (Aqua and Terra) significantly predicted PM_{10} ($\beta 1 = 249.807$, $p < .001$, and $\beta 1 = 212.747$, $p < .001$) (Eqs. 11 and 13). As can be seen from the scatterplots (Figs. 19 and 21) and simple linear regressions (Eqs. 12 and 14), the AOD (Aqua and Terra) was also a significant predictor of $PM_{2.5}$.

Comparison between OMI/Aura SO_2, NO_2, Aerosol Index, and in situ measurements

Figures 23 and 24 show scatter plot from OMI/Aura satellite and in situ measurements between 14 and 25 October 2019, in Kaunas city for NO_2 and SO_2 concentrations, respectively. As shown in the figures, a comparison between NO_2 and SO_2 derived from OMI/Aura and in situ measurements over the Kaunas city revealed a good correlation during the mentioned period. However, the OMI/Aura satellite product could provide a more accurate estimation and higher correlation coefficient value (0.89) for the concentration of SO_2 pollutants than NO_2.

Linear regression analysis was performed to find the correlation between the Aura (OMI) retrieved SO_2 and NO_2 values and in situ SO_2 and NO_2 concentration, and the resultant equations were as follows:

$$NO_{2\ \text{In-Situ}} = 17.572 + 2.029 * NO_{2\ \text{OMI/Aura}} \quad (15)$$

$$SO_{2\ \text{In-Situ}} = 5.273 + 1.262 * SO_{2\ \text{OMI/Aura}} \quad (16)$$

Simple linear regression was carried out to investigate the relationship between OMI (Aura) retrieved NO_2 and SO_2 values ($\mu g/m^3$) and in situ NO_2 and SO_2 concentration ($\mu g/m^3$). The scatterplot (Figs. 23 and 24) showed that there was a

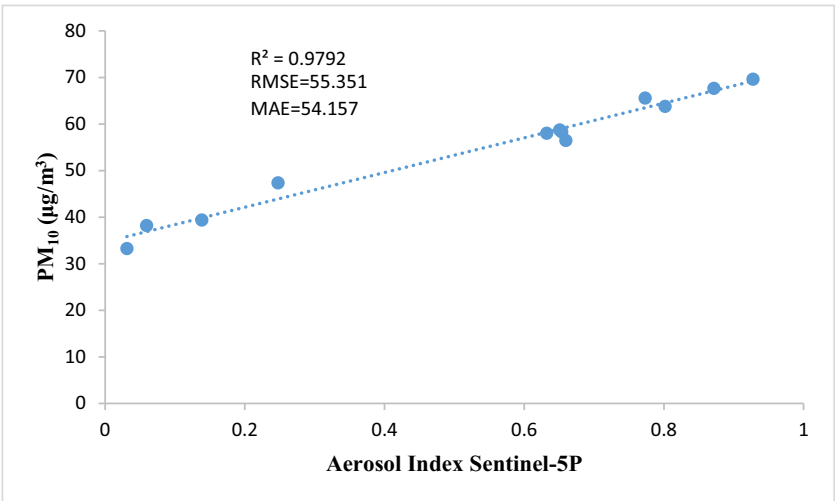

Fig. 17 Linear relation of Sentinel-5P/NRTI Aerosol Index and in situ PM_{10} concentration

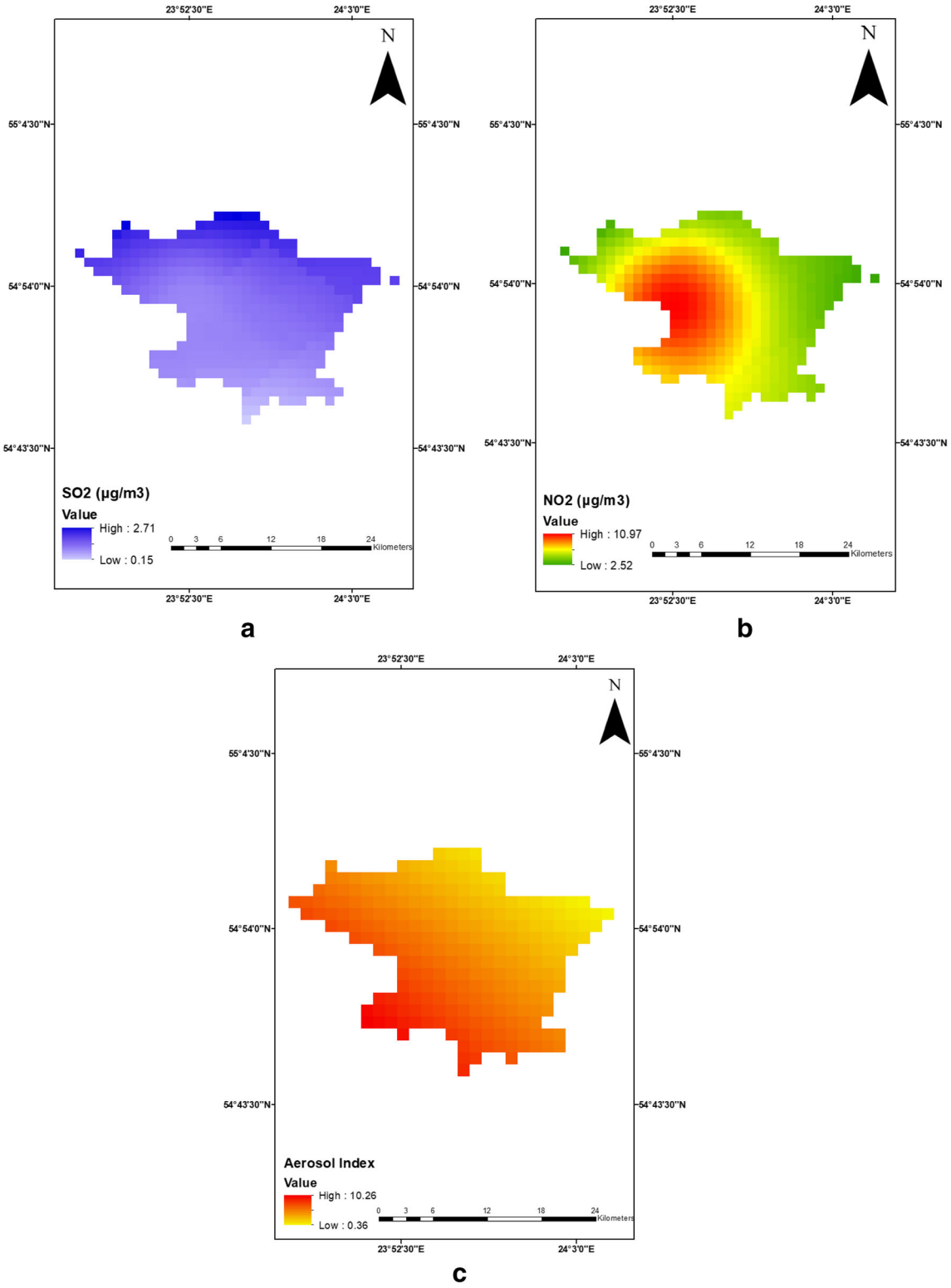

Fig. 18 Spatial distribution of the (**a**) SO_2 concentration, (**b**) NO_2 concentration, and (**c**) Aerosol Index (OMI/Aura) during 14 through 25 October 2019 at Kaunas city

positive linear relationship between the two, which was confirmed with Pearson's correlation coefficient of 0.791 and 0.945 for NO_2 and SO_2 OMI (Aura), respectively. Simple linear regression showed a significant relationship between OMI (Aura) retrieved SO_2 values and in situ SO_2 concentration ($p < 0.001$). The slope coefficient for in situ SO_2 concentration was 1.262, so the OMI (Aura) retrieved SO_2 values increases by 1.262 µg/m^3 for each extra µg/m^3 of in situ

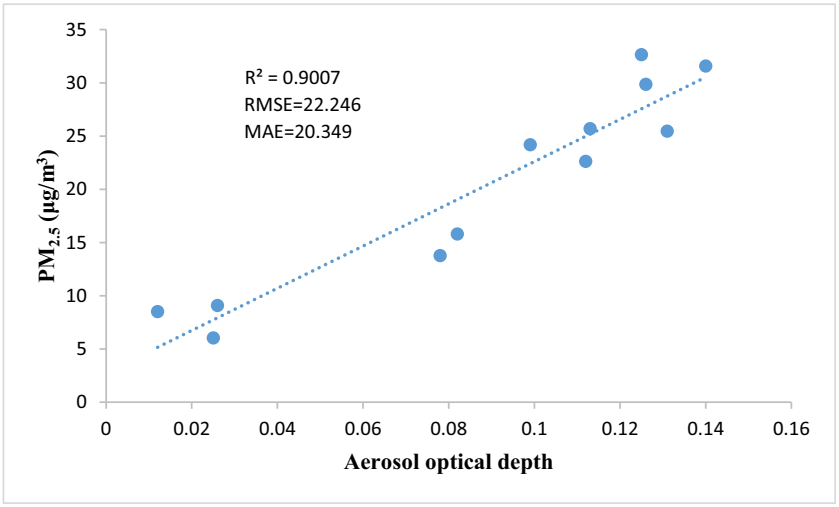

Fig. 19 Linear relation of MODIS/Aqua aerosol optical depth and in situ $PM_{2.5}$ concentration

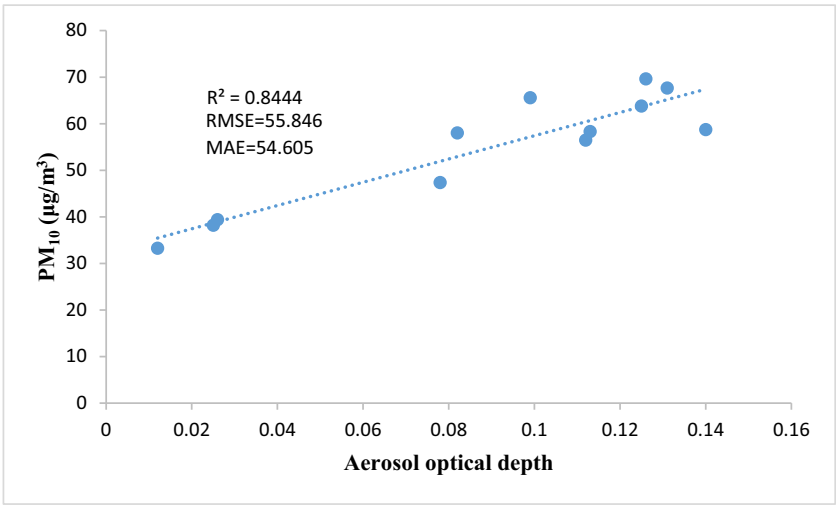

Fig. 20 Linear relation of MODIS/Aqua aerosol optical depth and in situ PM_{10} concentration

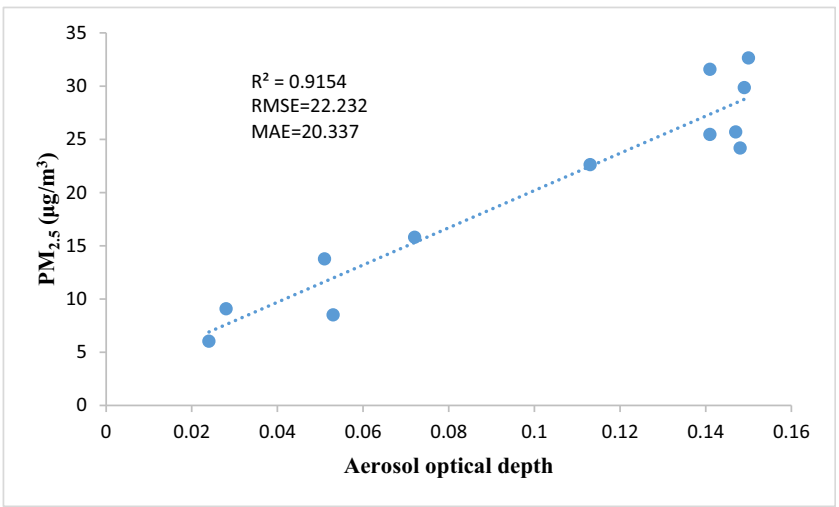

Fig. 21 Linear relation of MODIS/Terra aerosol optical depth and in situ $PM_{2.5}$ concentration

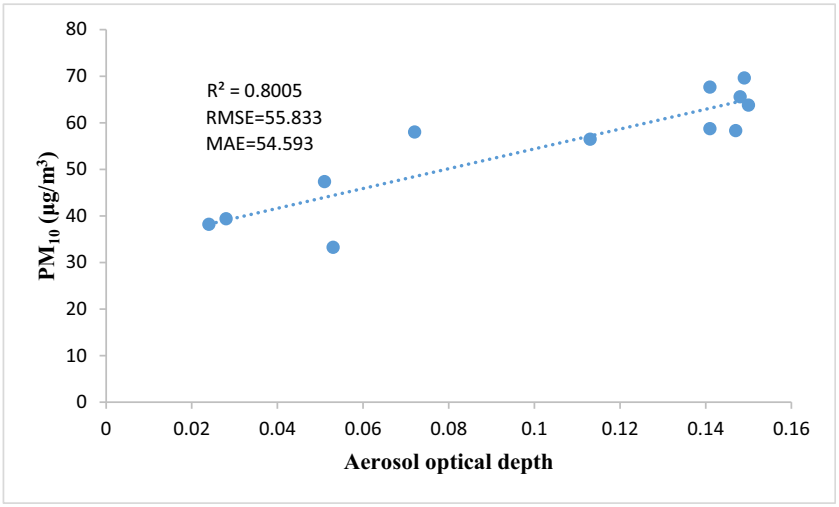

Fig. 22 Linear relation of MODIS/Terra aerosol optical depth and in situ PM_{10} concentration

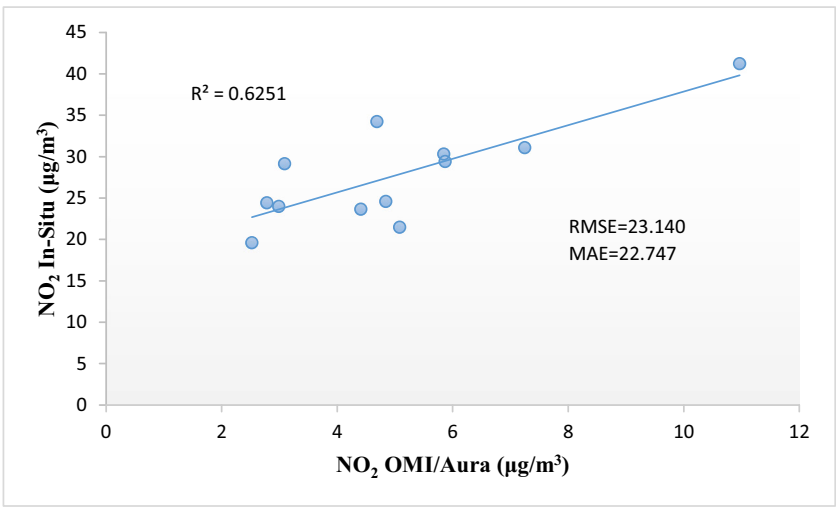

Fig. 23 Linear relation of OMI/Aura NO_2 and in situ NO_2 concentration

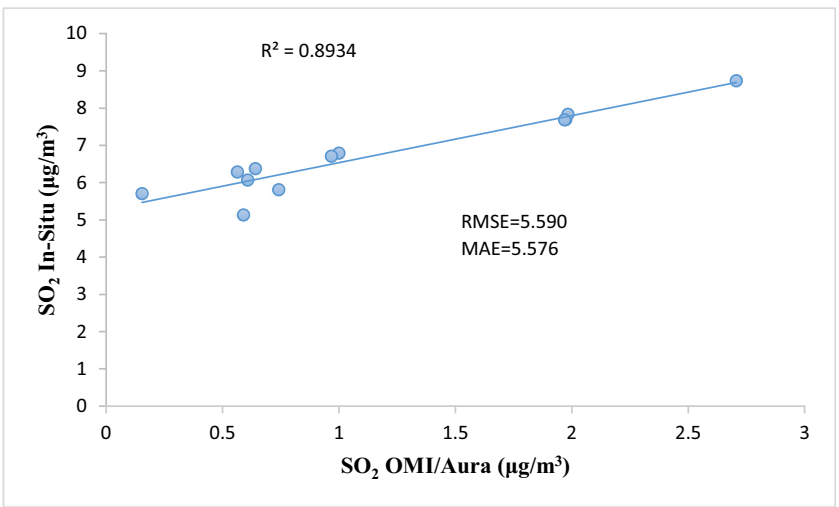

Fig. 24 Linear relation of OMI/Aura SO_2 and in situ SO_2 concentration

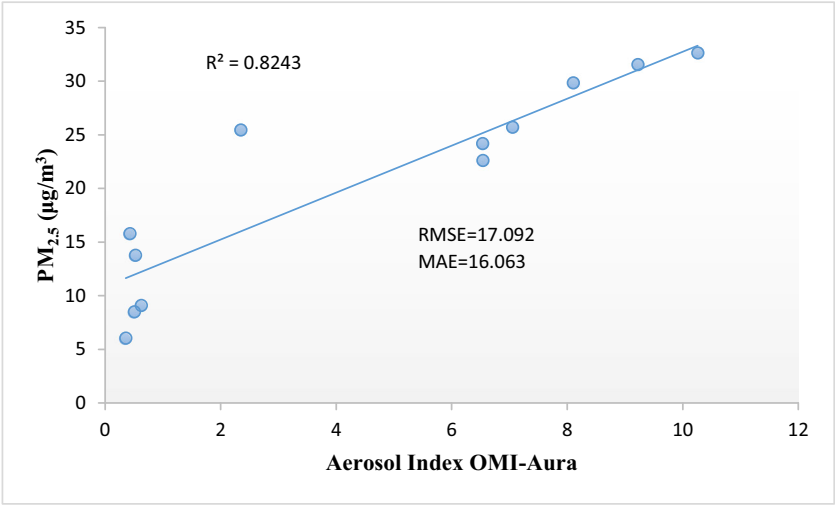

Fig. 25 Linear relation of OMI/Aura Aerosol Index and in situ $PM_{2.5}$ concentration

SO_2 concentration. The R^2 value was 0.893, so 89.3%, of the variation in in situ SO_2 concentration, can be explained by the model containing only SO_2 OMI (Aura). Also, the R^2 value was 0.625, so 62.5%, of the variation in in situ NO_2 concentration, can be explained by the model containing only NO_2 OMI (Aura).

Figures 25 and 26 show the scatter plot between the Aerosol Index from OMI/Aura satellite and in situ measurements of PM from 14 to 25 October 2019 in Kaunas city. A high correlation coefficient value (0.82) shows that there is a strong and positive correlation between the two parameters (Fig. 25). Linear regression analysis was performed between the Aura (OMI) retrieved AI values and PM ($PM_{2.5}$ and PM_{10}) observations, and the equations were:

$$PM_{10} = 45.298 + 2.147*AI_{OMI/Aura} \quad (17)$$

$$PM_{2.5} = 10.859 + 2.189*AI_{OMI/Aura} \quad (18)$$

A simple linear regression was calculated to predict in situ PM_{10} and $PM_{2.5}$ concentration based on AI values from OMI (Aura). Significant regression equations were found ($F(1,10) = 8.820$, $p < 0.05$), with a R^2 of 0.469 for PM_{10} and AI and ($F(1,10) = 46.919$, $p < 0.001$), with a R^2 of 0.824 for $PM_{2.5}$ and AI. PM_{10} concentration increased 2.147 for each of the AI (Eq. 17). $PM_{2.5}$ concentration increased 2.189 for each of the AI (Eq. 18).

Finally, we calculated the percentage difference for every satellite data and ground station. Results illustrated that SO_2 and NO_2 pollutants between Sentinel-5P and in situ 21% and 10% and for OMI (Aura) 44% and 60%, respectively, are differences. Also, the percentage difference is between MODIS AOD (Aqua and Terra) in situ particulate matter (PM) are 19.85% and 19.9%, respectively, and also for OMI (Aura) and Sentinel 5P AI, 15.95% and 19.30%, respectively.

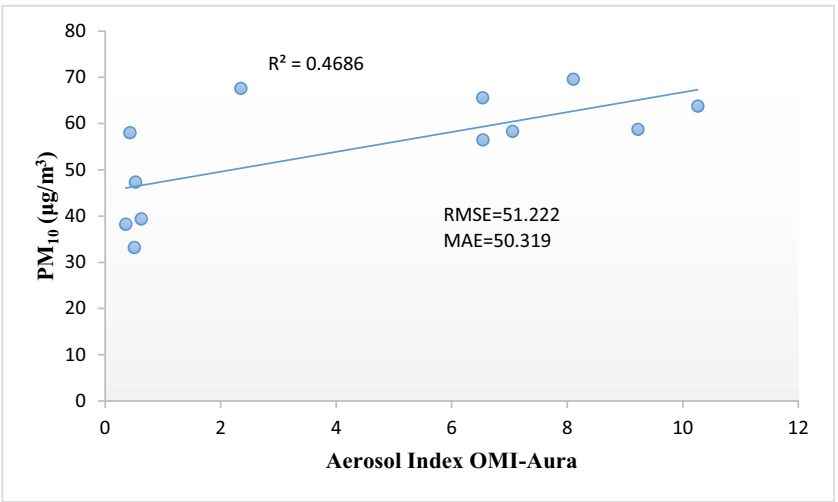

Fig. 26 Linear relation of OMI/Aura Aerosol Index and in situ PM_{10} concentration

Conclusions

In this study, the relation between air pollutants, SO_2, NO_2, and PM (PM_{10} and $PM_{2.5}$), remotely sensed data retrieved from the Sentinel-5P, OMI (Aura), and MODIS (Aqua and Terra) over the Kaunas city during the period 14–25 October 2019, when tire recycling manufactory fire occurred in the Alytus, and geographic information system has been investigated. Remotely sensed data, such as MODIS AOD, Sentinel-5P, and OMI/Aura air pollutants, are valuable tools to be used in air quality applications. Comparison between air pollutants derived from different satellite products and in situ observations over the Kaunas city during the 12 days of autumn 2019 (14–25 October) when the fire of a tire recycling manufactory in the Alytus occurred revealed good correlations.

According to analysis and results, it can be said that the Terra, Aqua, OMI (Aura), and Sentinel-5P satellites are all approximately equally well to be useful for detecting localized PM (PM_{10} and $PM_{2.5}$) pollution. Also, it can be said that the Sentinel-5P satellite was able to detect air pollutants such as SO_2 and NO_2 better than Aura during the study period. The higher spatial resolution of the Sentinel-5P satellite could be the reason for the sensor's high ability to estimate the number of air pollutants being studied. That being said, the Sentinel-5P's higher resolution allows it to match up better with localized pollution sources measured.

The overall results of this study confirmed the capability of Sentinel-5P data to be used in monitoring the air quality and air pollution over the Kaunas local area. The existence of strong and acceptable correlations between satellite data and in situ measurements was indicative of the ability of satellite images to monitor air pollution, particularly over Kaunas urban areas during the fire incident in the city of Alytus. Finally, it was demonstrated that the spatial distribution of the air pollutants could be mapped from remotely sensed data, accurately.

References

Alston EJ, Sokolik IN, Doddridge BG (2011) Investigation into the use of satellite data in aiding characterization of particulate air quality in the Atlanta, Georgia metropolitan area. J Air Waste Manage Assoc 61(2):211–225. https://doi.org/10.3155/1047-3289.61.2.211

Barkley MP, Abad GG, Kurosu TP, Robert Spurr R, Torbatian S, Lerot C (2017) OMI air-quality monitoring over the middle east. Atmos Chem Phys 17:4687–4709. https://doi.org/10.5194/acp-17-4687-2017

Bechle MJ, Millet DB, Marshall JD (2012) Remote sensing of exposure to NO2: satellite versus ground-based measurement in a large urban area. Atmos Environ 69:345–353. https://doi.org/10.1016/j.atmosenv.2012.11.046

Brook RD, Newby DE, Rajagopalan S (2017) The global threat of outdoor ambient air pollution to cardiovascular health: time for intervention. JAMA Cardiol 2:353–354. https://doi.org/10.1001/jamacardio.2017.0032

Brunekreef B, Holgate ST (2002) Air pollution and health. Lancet 360: 1233–1242

Carn SA, Krueger AJ, Krotkov NA, Yang K, Levelt PF (2007) Sulfur dioxide emissions from Peruvian copper smelters detected by the ozone monitoring instrument. Geophys Res Lett 34:L09801. https://doi.org/10.1029/2006GL029020

Celarier EA et al (2008) Validation of Ozone monitoring instrument nitrogen dioxide columns. Geophys Res 113:D15S15. https://doi.org/10.1029/2007JD008908

Chen W, Wang H, Zhao H, Qin K (2020) Google Earth Engine–assisted black carbon radiative forcing calculation over a heavy industrial city in China. Air Qual Atmos Health 13:329–338. https://doi.org/10.1007/s11869-020-00796-9

Chu DA, Kaufman YJ, Zibordi G, Chern JD, Mao J, Li C, Holben BN (2003) Global monitoring of air pollution over land from the Earth observing system-Terra moderate resolution imaging spectroradiometer (MODIS). Geophys Res 108:4661. https://doi.org/10.1029/2002JD003179

Chu Y, Liu Y, Li X, Liu Z, Lu H, Lu Y, Liu F (2016) A review on predicting ground $PM_{2.5}$ concentration using satellite aerosol optical depth. Atmosphere 7(10):129. https://doi.org/10.3390/atmos7100129

Clark LP, Millet DB, Marshall JD (2014) National patterns in environmental injustice and in-equality: outdoor NO2 air pollution in the United States. PLoS One 9:e94431. https://doi.org/10.1371/journal.pone.0094431

De Smedt I, Stavrakou T, Müller JF, van der ARJ, Van Roozendael M (2010) Trend detection in satellite observations of formaldehyde tropospheric columns. Geophys Res Lett 37:L18808. https://doi.org/10.1029/2010GL044245

De Smedt I, Stavrakou T, Hendrick F, Danckaert T, Vlemmix T, Pinardi G, Theys N, Lerot C, Gielen C, Vigouroux C, Hermans C, Fayt C, Veefkind P, Müller JF, Van Roozendael M (2015) Diurnal, seasonal and long-term variations of global formaldehyde columns inferred from combined OMI and GOME-2 observations. Atmos Chem Phys 15:12519–12545. https://doi.org/10.5194/acp-15-12519-2015

Duncan BN, Prados AI, Lamsal LN, Liu Y, Streets DG, Gupta P, Hilsenrath E, Kahn RA, Nielsen JE, Beyersdorf AJ, Burton SP, Fiore AM, Fishman J, Henze DK, Hostetler CA, Krotkov NA, Lee P, Lin M, Pawson S, Pfister G, Pickering KE, Pierce RB, Yoshida Y, Ziemba LD (2014) Satellite data of atmospheric pollution for U.S. air quality applications: Examples of applications, summary of data end-user resources, answers to FAQs, and common mistakes to avoid. Atmos Environ 94:647–662. https://doi.org/10.1016/j.atmosenv.2014.05.061

Duncan BN, Lamsal LN, Thompson AM, Yoshida Y, Lu Z, Streets DG, Hurwitz MM, Pickering KE (2016) A spacebased, high-resolution view of notable changes in urban NOx pollution around the world (2005–2014). Geophys Res 121:976–996. https://doi.org/10.1002/2015JD024121

El-Nadry M, Li W, El-Askary HA, Awad MA, Mostafa AR (2019) Urban health related air quality indicators over the Middle East and North Africa countries using multiple satellites and AERONET Data. Remote Sens 11:2096. https://doi.org/10.3390/rs11182096 1-24

Emili E, Popp C, Petitta M, Riffler M, Wunderle S, Zebisch M (2010) PM_{10} remote sensing from geostationary SEVIRI and polar-orbiting MODIS sensors over the complex terrain of the European Alpine region. Remote Sens Environ 114(11):2485–2499. https://doi.org/10.1016/j.rse.2010.05.024

Evans KA, Halterman JS, Hopke PK, Fagnano M, Rich DQ (2014) Increased ultrafine particles and carbon monoxide concentrations are associated with asthma exacerbation among urban children. Environ Res 129:11–19. https://doi.org/10.1016/j.envres.2013.12.001

Ghude SD, Fadnavis S, Beig G, Polade SD, van der ARJ (2008) Detection of surface emission hot spots, trends, and seasonal cycle

from satellite-retrieved NO2 over India. Geophys Res 113:D20305. https://doi.org/10.1029/2007JD009615

Gorelick N, Hancher M, Dixon M, Ilyushchenko S, Thau D, Moore R (2017) Google earth engine: planetary-scale geospatial analysis for everyone. Remote Sens Environ 202:18–27. https://doi.org/10.1016/j.rse.2017.06.031

Hilboll A, Richter A, Burrows JP (2013) Long-term changes of tropospheric NO2 over megacities derived from multiple satellite instruments. Atmos Chem Phys 13:4145–4169. https://doi.org/10.5194/acp-13-4145-2013

Hoek G, Krishnan RM, Beelen R, Peters A, Ostro B, Brunekreef B, Kaufman JD (2013) Long-term air pollution exposure and cardio-respiratory mortality: a review. Environ Health 12:1–15. https://doi.org/10.1186/1476-069X-12-43

Hsu NC (2017) Changes to MODIS Deep Blue aerosol products between collection 6 and collection 6.1. https://modis-atmosphere.gsfc.nasa.gov/sites/default/files/ModAtmo/modis_deep_blue_c61_changes2.pdf. Accessed 24 July 2017

Hsu NC, Tsay SC, King MD, Herman JR (2004) Aerosol properties over bright-reflecting source regions. IEEE Trans Geosci Remote Sens 42(3557):3569–3569. https://doi.org/10.1109/TGRS.2004.824067

Hsu NC, Jeong MJ, Bettenhausen C, Sayer AM, Hansell R, Seftor CS, Tsay SC (2013) Enhanced Deep Blue aerosol retrieval algorithm: the second generation. Geophys Res Atmos 118:169296–169315. https://doi.org/10.1002/jgrd.50712

Jin X, Holloway T (2015) Spatial and temporal variability of ozone sensitivity over China observed from the ozone monitoring instrument. Geophys Res 120:7229–7246. https://doi.org/10.1002/2015JD023250

King MD, Kaufman YJ, Menzel WP, Tanre D (1992) Remote-sensing of cloud, aerosol, and water-vapor properties from the moderate resolution imaging spectrometer (Modis). IEEE Trans Geosci Remote Sens 30:2–27. https://doi.org/10.1109/36.124212

Koelemeijer RBA, Homan CD, Matthijsen J (2006) Comparison of spatial and temporal variations of aerosol optical thickness and particulate matter over Europe. Atmos Environ 40(27):5304–5315. https://doi.org/10.1016/j.atmosenv.2006.04.044

Krotkov NA, McClure B, Dickerson RR, Carn SA, Li C, Bhartia PK, Yang K, Krueger AJ, Li Z, Levelt P, Chen H, Wang P, Lu DR (2008) Validation of SO2 retrievals from the ozone monitoring instrument over NE China. Geophys Res 113:D16S40. https://doi.org/10.1029/2007JD008818

Krotkov NA, McLinden CA, Li C, Lamsal LN, Celarier EA, Marchenko SV, Swartz WH, Bucsela EJ, Joiner J, Duncan BN, Boersma KF, Veefkind JP, Levelt PF, Fioletov VE, Dickerson RR, He H, Lu Z, Streets DG (2016) Aura OMI observations of regional SO2 and NO2 pollution changes from 2005 to 2015. Atmos Chem Phys 16:4605–4629. https://doi.org/10.5194/acp-16-4605-2016

Lamsal LN, Martin RV, van Donkelaar A, Steinbacher M, Celarier EA, Bucsela E, Dunlea EJ, Pinto JP (2008) Ground-level nitrogen dioxide concentrations inferred from the satellite-borne Ozone Monitoring Instrument. Geophys Res 113. https://doi.org/10.1029/2007JD009235

Lamsal LN, Duncan BN, Yoshida Y, Krotkov NA, Pickering KE, Streets DG, Lu Z (2015) U.S. NO2 trends (2005–2013): EPA air quality system (AQS) data versus improved observations from the ozone monitoring instrument (OMI). Atmos Environ 110:130–143. https://doi.org/10.1016/j.atmosenv.2015.03.055

Lelieveld J, Beirle S, Hörmann C, Stenchikov G, Wagner T (2015) Abrupt recent trend changes in atmospheric nitrogen dioxide over the Middle East. Sci Adv 1:e1500498. https://doi.org/10.1126/sciadv.1500498

Liu Y, Saranat JA, Kilaru V, Jacob DJ, Koutrakis P (2005) Estimating ground-level PM2.5 eastern United States using satellite remote sensing. Environ Sci Technol 39:3269–3278. https://doi.org/10.1021/es049352m

Liu Y, Paciorek CJ, Koutrakis P (2009) Estimating regional spatial and temporal variability of PM2.5 concentrations using satellite data, meteorology, and land use information. Environ Health Perspect 117:886e892–886e892. https://doi.org/10.1289/ehp.0800123

Liu Z, Ostrenga D, Teng W, Kempler S (2013) Developing online visualization and analysis services for NASA satellite-derived global precipitation products during the Big Geospatial Data Era. Ch. 5, in Big GeoSpatial Data. 89–114. https://doi.org/10.1201/b16524-6

Martin R (2008) Satellite remote sensing of surface air quality. Atmos Environ 42:7823e7843–7823e7843. https://doi.org/10.1016/j.atmosenv.2008.07.018

Prados AI, Leptoukh G, Lynnes C, Johnson J, Rui H, Chen A, Husar RB (2010) Access, visualization, and interoperability of air quality remote sensing data sets via the Giovanni online tool. IEEE J Sel Top Appl Earth Obs Remote Sens 3(3):359–370. https://doi.org/10.1109/JSTARS.2010.2047940

Putrenko VV Pashynska NM. (2017) The use of remote sensing data for modeling air quality in the cities. ISPRS Annals of the Photogrammetry, Remote Sensing and Spatial Information Sciences, Volume IV-5/W1, 2017 Geospace. https://doi.org/10.5194/isprs-annals-IV-5-W1-57-2017

Richter A, Burrows JP, Nüß H, Granier C, Niemeier U (2005) Increase in tropospheric nitrogen dioxide over China observed from space. Nature 437:129–132. https://doi.org/10.1038/nature04092

Rohen GJ, von Hoyningen-Huene W, Kokhanovsky A, Dinter T, Vountas M, Burrows JP (2011) Retrieval of aerosol mass load (PM10) from MERIS/Envisat top of atmosphere spectral reflectance measurements over Germany. Atmos Meas Tech 4:523–534. https://doi.org/10.5194/amt-4-523-2011

Russell AR, Valin LC, Cohen RC (2012) Trends in OMI NO2 observations over the United States: effects of emission control technology and the economic recession. Atmos Chem Phys 12:12197–12209. https://doi.org/10.5194/acp-12-12197-2012

Safarianzengir V, Sobhani B, Yazdani MH, Kianian M (2020) Monitoring, analysis and spatial and temporal zoning of air pollution (carbon monoxide) using Sentinel-5 satellite data for health management in Iran, located in the Middle East. Air Qual Atmos Health 13:709–719. https://doi.org/10.1007/s11869-020-00827-5

Schneider P, van der ARJ (2012) A global single-sensor analysis of 2002–2011 tropospheric nitrogen dioxide trends observed from space. Geophys Res 117:d16309. https://doi.org/10.1029/2012JD017571

Schneider P, Lahoz WA, van der AR (2015) Recent satellite-based trends of tropospheric nitrogen dioxide over large urban agglomerations worldwide. Atmos Chem Phys 15:1205–1220. https://doi.org/10.5194/acp-15-1205-2015

Slagter B, Tsendbazar NE, Vollrath A, Reiche J (2020) Mapping wetland characteristics using temporally dense Sentinel-1 and Sentinel-2 data: a case study in the St. Lucia wetlands, South Africa. Int J Appl Earth Obs Geoinf 86:141–189. https://doi.org/10.1016/j.jag.2019.102009

Streets DG, Canty T, Carmichael GR, de Foy B, Dickerson RR, Duncan BN, Edwards DP, Haynes JA, Henze DK, Houyoux MR, Jacob DJ, Krotkov NA, Lamsal LN, Liu Y, Lu Z, Martin RV, Pfister GG, Pinder RW, Salawitch RJ, Wecht KJ (2013) Emissions estimation from satellite retrievals: a review of current capability. Atmos Environ 77:1011–1042. https://doi.org/10.1016/j.atmosenv.2013.05.051

Tatem AJ, Goetz SJ, Hay SI (2004) Terra and Aqua: new data for epidemiology and public health. Int J Appl Earth Obs Geoinf 6:33–46. https://doi.org/10.1016/j.jag.2004.07.001

Tsai TC, Jeng YJ, Chu DA, Chen JP, Chang SC (2011) Analysis of the relationship between Modis aerosol optical depth and particulate matter from 2006 to 2008. Atmos Environ 45:1–12. https://doi.org/10.1016/j.atmosenv.2009.10.006

Usmani RSA, Saeed A, Abdullahi AM, Pillai TR, Jhanjhi NZ, Hashem IAT (2020) Air pollution and its health impacts in Malaysia: a review. Air Qual Atmos Health 13:1093–1118. https://doi.org/10.1007/s11869-020-00867-x

van der ARJ, Peters DHMU, Eskes H, Boersma KF, Van Roozendael M, De Smedt I, Kelder HM (2006) Detection of the trend and seasonal variation in tropospheric NO2 over China. Geophys Res 111: D12317. https://doi.org/10.1029/2005JD006594

van der ARJ, Eskes HJ, Boersma KF, van Noije TPC, Van Roozendael M, De Smedt I, DHMU P, Meijer EW (2008) Trends, seasonal variability and dominant NOx source derived from a ten year record of NO_2 measured from space. Geophys Res 113:d04302. https://doi.org/10.1029/2007JD009021

Wang J, Christopher SA (2003) Intercomparison between satellite-derived aerosol optical thickness and $PM_{2.5}$ mass: implications for air quality studies. Geophys Res Lett 30:2095. https://doi.org/10.1029/2003GL018174

Wang Y, Wang J, Zhou M, Daven K, Henze DK, Ge C, Wang W (2020) Inverse modeling of SO2 and NOx emissions over China using multisensor satellite data- part 2. Downscaling techniques for air quality analysis and forecasts. Atmos Chem Phys 20:1–38. https://doi.org/10.5194/acp-20-6651-2020